CHAPTER 2

Theory

There are many theories which related to the star formation study via Hα detection. This is absolutely essential to have an understanding of these basic principles. They can be used in the research methodology and to explain various phenomena occurring within galaxies as well as the evolution of galaxies in galaxy groups.

2.1 Galaxy Groups, Clusters and Superclusters

Our Galaxy is surrounded by billions of other galaxies spread throughout space. Many galaxies are combined into galaxy groups or galaxy clusters. For example, our Milky Way is one of galaxy members in the Local Group. It has about a few dozen satellite galaxies, including two especially dominant ones: the Large Magellanic Cloud (LMC) and Small Magellanic Cloud (SMC). The nearby largest Local Group galaxy is Andromeda Galaxy (M31). This spiral galaxy (type Sb) is more massive than the Milky Way and locates at a distance of 0.8 Mpc. In total, the Local Group has approximately 30 galaxies (Jones et al., 2004). Typically, galaxy groups have about 1.2 Mpc in radius and include with fewer than 50 members. The groups with more than about 50 galaxy members are called galaxy clusters which have radius of about 2-5 Mpc. The small clusters are called open, diffuse, or irregular clusters which have hundreds of galaxies, diameters less than 10 Mpc and a total mass of $10^{12} - 10^{14}$ $M_{\odot}$. The large clusters are called rich, or regular cluster, with thousands of galaxies, diameters up to 10 Mpc and total mass of about 10^{15} $M_{\odot}$ (Phillipps, 2005). Virgo Cluster, for example, which is about 15 Mpc distant. It is much more irregular in shape, and contains a mixture of ellipticals and spirals. While the Coma Cluster at distance of about 90 Mpc from our Galaxy. It is spherical symmetrical cluster consisting mainly of elliptical galaxies (Jones et al., 2004). Both the Coma and the Virgo clusters contain over a thousand galaxies as shown in figure 2.1. If some galaxies, groups, or clusters form a lager system with a radius of 5-10 Mpc approximately, they

are called superclusters (Bennett et al., 2012; Karttunen et al., 2007). Although galaxy clusters consist of many galaxies, but some galaxies are not reside in the clusters. We call those galaxies as field galaxies. We must bewared to identify and exclude them from the cluster surveys.

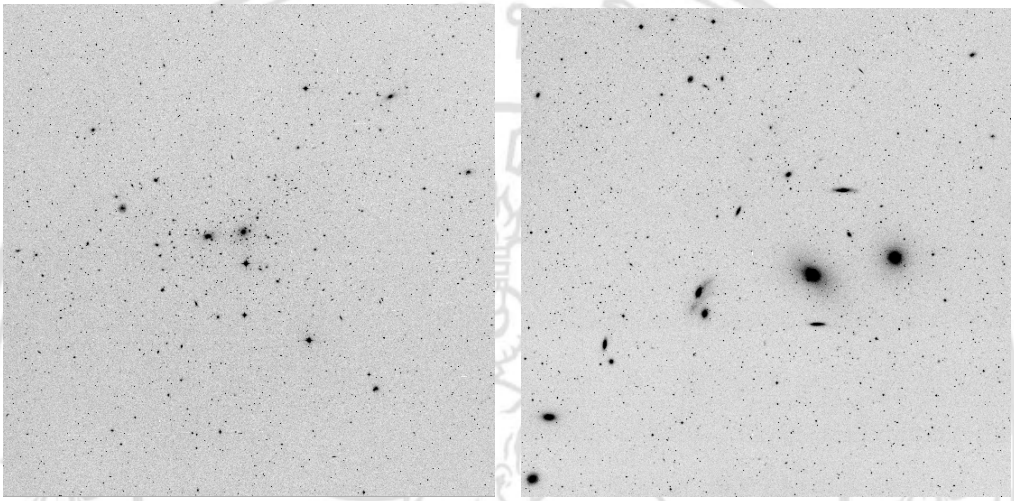

(a) (b)

Figure 2.1: Optical image of galaxy clusters from ESO-DSS. (a) The Coma cluster and (b) The Virgo cluster.

2.2 Morphological Type and T-type of Galaxies

In 1926 A.D. the American astronomer, Edwin P. Hubble has studied many galaxies in the universe and invented a system for galaxy classification, according to their visual morphology as elliptical, spiral, barred spiral, lenticular and irregular types. The first four kinds of galaxies can be arranged in Hubble's tuning fork diagram as shown in figure 2.2.

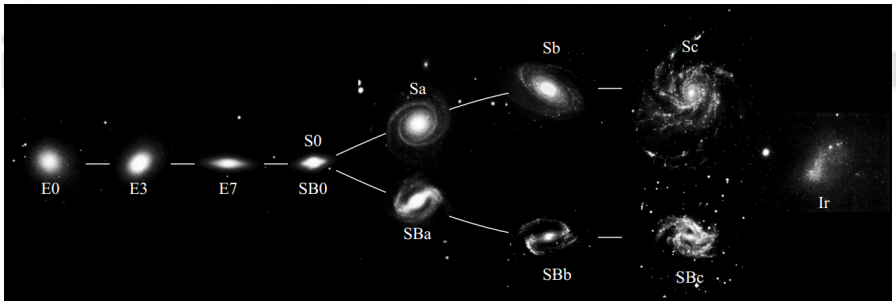

Figure 2.2: Hubble's tuning fork diagram (Carroll and Ostlie, 2014).

On the handle of Hubble tuning fork at the left, elliptical galaxies are arranged, designated by the letter E and a number represented ellipticity. E0 galaxy is a sphere, and the highest elongated type is defined by E7, and we call such galaxies as early-type. The two forks show spiral galaxies called late-type, assigned by the letter S for regular spirals and SB for barred spirals, followed by a lowercase a, b or c. The pitch angle of spiral arms increases from a to c, while the bulge size decreases, and at the middle of the fork shows lenticular galaxies, which are designated as S0 (Bennett et al., 2012).

T-type is a number used to determine the type and morphology of the galaxies that defined by the French astronomer, de Vaucouleurs (1959). It ranges from –6 to 10, with negative number represent to early-types and positive numbers to late-types as shown in the table 2.1.

Table 2.1: Hubble morphological types and T-types (Binney and Merrifield, 1998).

T-type	de Vaucouleurs	approx. Hubble
-6	cE	
-5	E	E
-4	E^+	
-3	$S0^-$, $SB0^-$	
-2	$S0^0$, $SB0^0$	S0, SB0
-1	$S0^+$, $SB0^+$	
0	S0/a, SB0/a	S0/a, SB0/a
1	Sa, SBa	Sa, SBa
2	Sab, SBab	Sa-b, SBa-b
3	Sb, SBb	Sb, SBb
4	Sbc, SBbc	Sb-c, SBb-c
5	Sc, SBc	
6	Scd, SBcd	Sc, SBc
7	Sd, SBd	
8	Sdm	Sc-Irr
9	Sm	
10	Im	Irr I

de Vaucouleurs system is developed from Hubble classification of galaxy morphological types. The several subtypes are defined. For example, Sab and Sbc for the galaxy that is unclear to be classified into Sa or Sb and Sb or Sc, respectively. These numerical types are much convenience for analysis of correlations between the morphological types

against the quantitative parameters and physical properties of galaxies. The Hubble classification is important in galactic astronomy. Of course, there are physical properties and morphology differences between various types. There are several important questions to ask when determining the Hubble class and types defined, i.e. Is there any overall regularity or symmetry?, Is the light concentrated in the center?, Is there a disc? and Are there any spiral arms? (Jones et al., 2004). The answers of these questions will be explained in following sections.

2.2.1 Elliptical galaxies

Elliptical galaxies are classified by overall elliptical shape when observed in the sky. The light emitted mainly from the center of the galaxy and decreases with increasing distance from the center (see figure 2.3). The elliptical galaxies are denoted by the letter E and a number, n, represented ellipticity. The ellipticity (ϵ) is in a range from 0 to 1 and is defined by relative size of semimajor axis, a, and semiminor axis, b, as given by equation 2.1.

$$\epsilon = 1 - \frac{a}{b}. \tag{2.1}$$

The number, n, ranging 0 to 7 is obtained by multiplying the ellipticity by ten and is given by equation 2.2.

$$n = 10\left(1 - \frac{a}{b}\right). \tag{2.2}$$

E0 galaxy appears round, E5 galaxies has its major axis twice as long as its minor axis, and the highest elongated type defined by E7. A galaxy whose real ellipticity of 0.5 may be visible in any shape from E0 to E5, depending on its orientation to the observer line of sight (Elmegreen, 1998).

The elliptical galaxies have more complicated structures. They are though to be either oblate like a pancake, or prolate like a rugby ball, or all three axes differ in length, it shaped into a triaxial. Physical properties of elliptical galaxies cover a wide range value. Their blue absolute magnitude may be as faint as -8 or brighter than -23, with a mass vary from $10^7 - 10^{13}$ $M_\odot$, and their diameter can be small as tens kpc and up to hundreds kpc. While dwarf elliptical galaxies have a mass only one-tenth or one-hundredth of a normal

elliptical. Their size are comparable to only a general globular cluster. dE is used to denote the dwarf elliptical galaxies (Carroll and Ostlie, 2014).

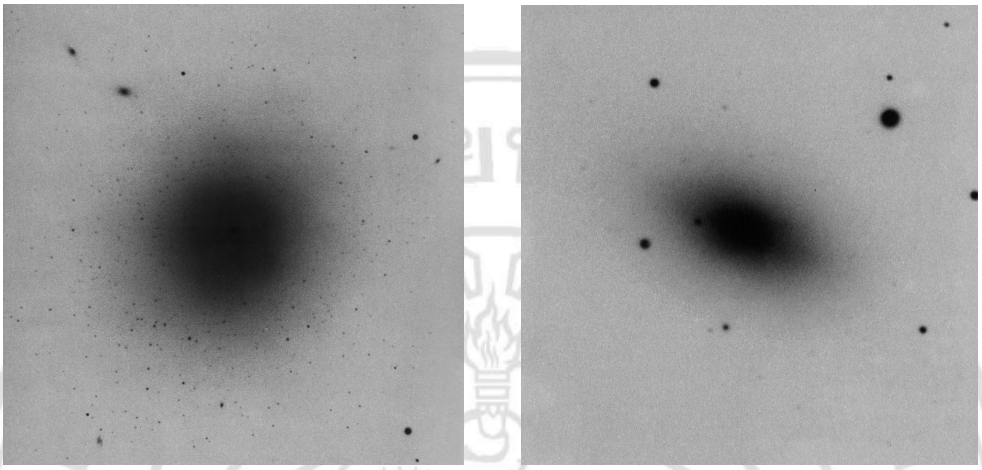

(a) (b)

Figure 2.3: Optical image of elliptical galaxies from ESO-DSS. (a) M87 (E0/1) and (b) NGC 4697 (E5).

Typically, the elliptical galaxies comprise little dust or cool gas. However, some giant elliptical galaxies are included of very hot gas. That low density and X-ray emitting gas is much like the gas in the hot bubble that is generated by supernova and powerful stellar wind in the galaxies. The deficiency of cold gas in elliptical galaxies designate that they have little or no taking place star formation. So, the elliptical galaxies appear red or yellow because they have no any hot, young, blue stars found in the disks of spiral galaxies (Bennett et al., 2012).

2.2.2 Lenticular galaxies

Lenticular (lenticular means "lens-shaped") galaxies are designated as S0, arranged at the middle of Hubble's tuning fork (Bennett et al., 2012). They have disk and spheroidal components like spiral galaxies but appear to absence spiral arms. Dwarf S0 is called spheroidal galaxies and designated as dS0. The designation of lenticular galaxies include subscript numbers following the S0. The number represent to the existence of dust or bars. For non-barred lentucluar, the $S0_1$ refer to lenticular with no dust, until $S0_3$ is corresponding to dark band of dust absorption. Examples are shown in figure 2.4. For barred lenticulars, the $SB0_1$ is the galaxies have a bar barely emerging from the bulge, and $SB0_3$

galaxies have narrow and well-defined bars. Components of lenticular galaxy consist of the nucleus, bulge, lens and envelope, or halo (Elmegreen, 1998). These components are not dominant appeared in profiles of the light distributions. But the outer regions are obviously fainter than the inner regions. Consequently, such galaxies are conveniently observed by the eye on an image. Sometimes, these galaxies are respected an intermediate type between spiral and elliptical, because they tend to have slight cool gas than normal spirals but more than ellipticals. Moreover, the lenticular consist mostly of old low mass stars like elliptical galaxies and their current star formation rate is extremely small (Elmegreen, 1998; Bennett et al., 2012).

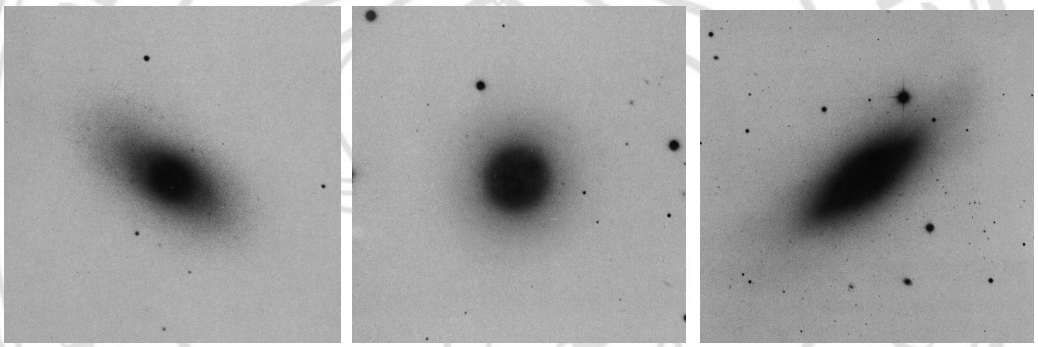

(a) (b) (c)

Figure 2.4: Optical image of lenticular galaxies from ESO-DSS. (a) NGC 1201 ($S0_1$), (b) NGC 524 ($S0_2$), and (c) NGC 5866 ($S0_3$).

2.2.3 Spiral galaxies

Spiral galaxies have bulges in the central regions, thin disks in the outer parts, and a halo surrounding these components. Typically, disks are thinner than the S0 galaxies and consist of gas and interstellar materials, where young stars are being born and form the spiral structure (Elmegreen, 1998; Karttunen et al., 2007). The classification system of spiral galaxy was developed by Hubble that depend on three parameters, i.e the bulge size relative to the disk length, the tightness of the spiral arms, and the degree of resolution of the disk into stars and H II regions. But always only the first two parameters are focused. The spiral galaxies (see figure 2.5) are arranged at the two Hubble's tuning forks called late-type, denoted by the letter S for normal spirals and SB for barred spirals, followed by a lowercase a, b, c, or d, for galaxies with large bulges and tight arms, down through

galaxies with small bulges and loose arms. Savchenko and Reshetnikov (2013) purposed that the tightly wound spiral arms are generated by the luminous and bright bulges. For example, the most dignified spiral galaxies, known as grand-design spirals, usually have two very symmetric and well-defined arms. The M51 (NGC 5194) is one of the best-known examples, shown in figure 2.6. However, there are many spiral galaxies whose spiral arms are difficult to well-defined, and called flocculent spirals.

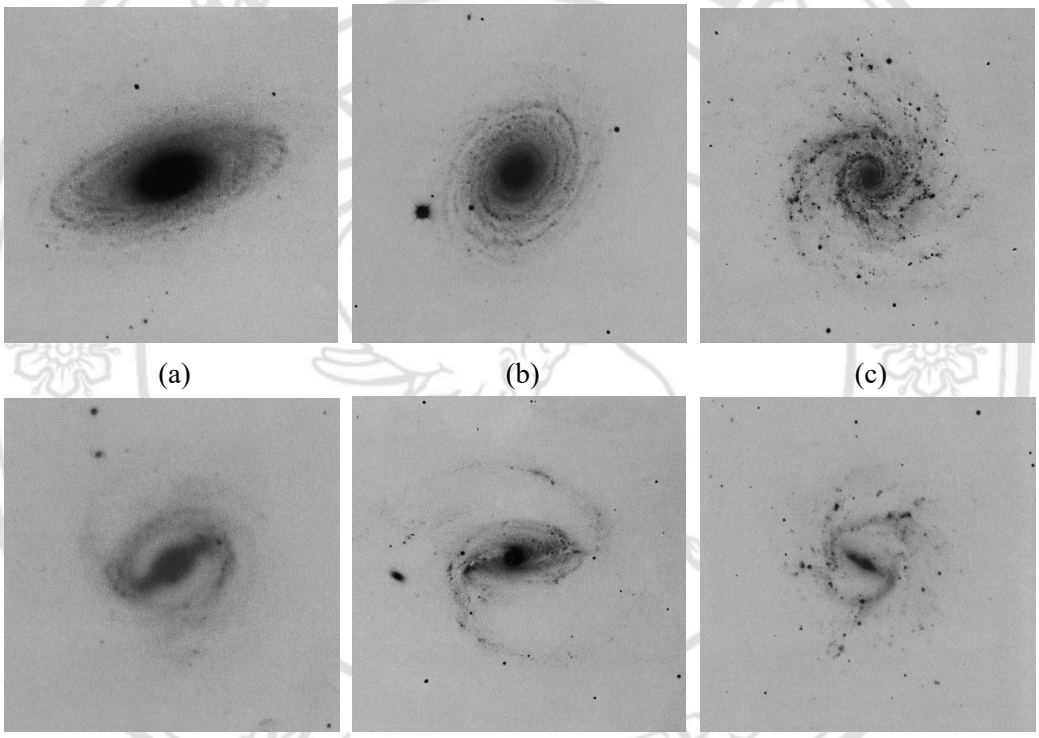

Figure 2.5: Optical image of spiral galaxies from ESO-DSS. (a) NGC 3898 (Sa), (b) NGC 488 (Sb), (c) NGC 628 (Sc), (d) NGC 175 (SBa), (e) NGC 1097 (SBb), and (f) NGC 1073 (SBc).

The tightness of the spiral arms can be defined by the pitch angle. This angle is the one of criterion to classify the morphological of spiral galaxies. The pitch angle is defined as the angle between the tangent to the spiral arm (solid line) and the perfect circle (dotted line), measured at the point where the arm and the circle intersect as shown in figure 2.7 (Carroll and Ostlie, 2014). The pitch angle can be in a range from about 5° in Sa type to about 20° in Sc type. Elmegreen (1998) informed that the important information about

the origin of the spiral structure in a particular galaxy can be analyzed from the variations in the pitch angle. In addition, the characteristic of galaxies, such as the shape of the surface brightness distribution of envelope-type or truncated disc galaxies, and the stellar disc color gradient were correlated with the variation of the pitch angle (Savchenko and Reshetnikov, 2013).

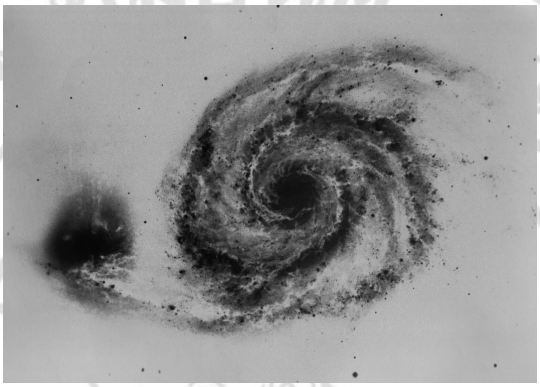

Figure 2.6: Optical image of grand-design-spiral galaxy (M51) from ESO-DSS.

Savchenko and Reshetnikov (2013) purposed that the spiral arm of galaxies cannot be explained by a single value of pitch angle. The other familiar criterion that used to categorize the spiral galaxies is bulge-to-disk luminosity ratio (B/D). The earliest type spirals (Sa or SBa) with the most prominent bulges and the smoothest distribution of stars in the arms have the largest (B/D),

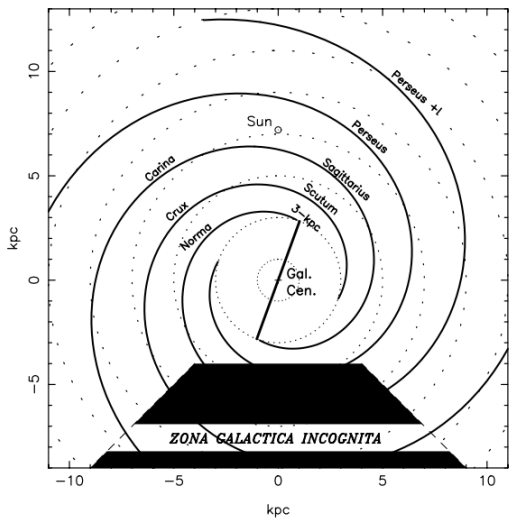

Figure 2.7: The pitch angle of a spiral arm (Vallée, 2002).

then decreasing to around 0.3 for Sb and to less than 0.1 for later type spirals. While Sd and Sm (Magellanic spiral) have no real bulge at all (Phillipps, 2005). However, Kennicutt (1981) demonstrated that the pitch angle of 113 spiral galaxies weakly correlate with arm structure and B/D, suggesting that Hubble classification criteria are less tightly coupled than previously believed.

The spiral galaxies also tend to be among the largest galaxies in the universe, with absolute B magnitudes from −16 to less than −23, masses between 10^9 to 10^{12} $M_\odot$, and disk diameters of 5 to 100 kpc. Because of spiral arm structure contains very luminous O and B main-sequence stars and H II regions. Thus the optical images of spiral galaxies are dominated by their arms. Since massive OB stars have a short-lived relative to the characteristic rotation period of a galaxy, spiral structure must correspond to regions of active star formation (Carroll and Ostlie, 2014). The early type spirals, Sa processed their gas more rapidly into stars, and so today are forming fewer stars. Their disks are redder and more metal-rich than those of Sc spirals (Elmegreen, 1998).

2.2.4 Irregular galaxies

The our nearest neighbor galaxies, i.e. LMC and SMC are categorized as irregular galaxies that appear to be in disarray. The figure 2.8 shows examples of irregular galaxies. The irregular galaxies tend to be smaller on average than ellipticals or spirals (Elmegreen, 1998).

Their shape do not fit easily into the previous designations of classification scheme. This class is divided into two types. Firstly, Type I irregular (Irr I, known as Im or Magellanic irregulars) which have low mass, slowly rotating system and do not have regular disk structure. They are rich in gas and comprise many young stars. Secondly, Type II irregular (Irr II) which is encountering intense starbursts, probably as a result of interactions (Elmegreen, 1998). Type Irr II are mainly contained dust, and resemble the irregular small ellipticals. Furthermore, both types of irregular galaxies are usually white and dusty, like the spiral disks because they contain young, massive stars. The detection by telescopic observations into the deep universe illustrate that distant galaxies are more similarly to be irregular than nearby galaxies. Due to the light that released from more distant galaxies

has taken longer to arrive the observer, these observations tell us that the younger universe could be mainly included these irregular galaxies (Bennett et al., 2012). Although the irregular galaxies tend to be particularly small but they have a wide range of specifications. Typically their absolute magnitudes in B band vary from −13 to −20, they have masses of between 10^8 and 10^{10} $M_\odot$, and their diameters range from 1 to 10 kpc (Carroll and Ostlie, 2014).

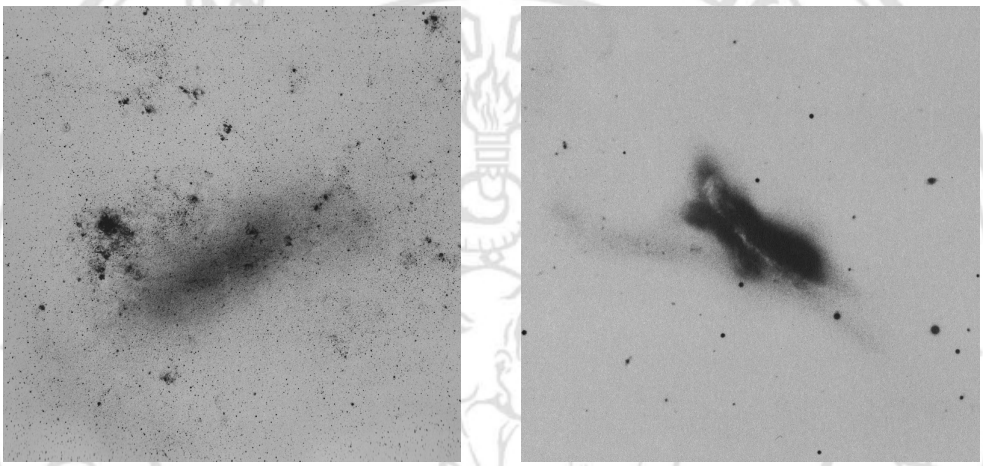

(a) (b)

Figure 2.8: Optical image of irregular galaxies from ESO-DSS. (a) Large Magellanic Cloud (Irr I) and (b) NGC 520 (Irr II).

2.3 Redshift and Peculiar Velocity

The words “redshift” and “blueshift” represent the displacement of the identifiable spectral lines. The wavelength of spectral lines will be shifted to shorter or longer than normal spectra observed base on standard laboratory conditions. One cause that shift can be arisen is Doppler effect, caused by the motion of the radiative source relative to the observer. In this case, the Doppler shift can be used to calculate the speed of the source which is receding or approaching the observer (Jones et al., 2004).

All distant galaxies spectra show redshift. Jones et al. (2004) demonstrated that these shifts are not simply the consequence of Doppler effect, but they arise from a change with time of the separation between us and the galaxies. A redshift corresponds to an increasing separation. The general definition of the redshift, z, is shown in equation 2.3

$$1 + z = \frac{\lambda_{\text{obs}}}{\lambda_{\text{em}}}, \tag{2.3}$$

where λ_{obs} is a value of observed wavelength and λ_{em} refers to known or emitted wavelength. If the relativistic effects are neglected in this simple derivation, we will have

$$z = \frac{\Delta\lambda}{\lambda_{\text{em}}} = \frac{v}{c}, \tag{2.4}$$

where $\Delta\lambda = \lambda_{\text{obs}} - \lambda_{\text{em}}$ is the change in wavelength observed for spectral line of a moving source at speed v and c is the speed of light in vacuum. Hubble (1929) purposed the first satisfied evidence of a linear relationship between the redshifts and distances of 24 sample galaxies, is given by

$$z = \frac{H_0}{c} d, \tag{2.5}$$

where H_0 is a proportional constant, known as the Hubble constant in unit km s^{-1} Mpc^{-1}. The relationship is explained by a cosmological principle, i.e. the universe is expanding. It is one of the pieces of evidence often quoted in contribute of the Big Bang theory. The motion of distant galaxies due merely to this expansion is known as the Hubble flow.

The ideal equation 2.5 (known as Hubble's Law) only applies over a small range of redshift, up to about 0.2 (Jones et al., 2004). The relationship between redshift and distance will be more complicated and not perfect linear relationship when the redshift increased. However, this equation can be used to interpreted the speed and distance of galaxies provided the redshift is adequately small.

The redshift measurement for a galaxy actually included of two components. The first one is the overall Hubble flow, which is the cluster's systemic velocity, and the second one is the peculiar velocity (v_{pec}), that is the gravitational effect of the cluster which will induce the peculiar motion of the galaxy inside the cluster (Phillipps, 2005). The peculiar velocity is defined as shown in the equation 2.6

$$v_{\text{pec}} = \frac{cz - cz_{\text{cl}}}{1 + z_{\text{cl}}} = \frac{v - v_{\text{cl}}}{1 + z_{\text{cl}}}, \tag{2.6}$$

where z_{cl} represents to the mean redshift, v_{cl} is the mean velocity of cluster galaxies.

2.4 Magnitude, Zero Point and Color Index

Most astronomical observations utilize electromagnetic radiation. We can obtain physical properties of electromagnetic sources via studying the energy distribution of radiation. When we observe the radiation source, that means we are measuring the energy accumulated during the period of time, which is equal to the integrated flux density over the area of the collecting detector in the period of time. If the source radiated isotropically, its radiation at a distance r is emanated on a spherical surface whose area is $4\pi r^2$ (Karttunen et al., 2007). If the flux density passing through this surface is f, The total flux (luminosity) is

$$L = 4\pi r^2 f. \tag{2.7}$$

Due to the response of the human eye to the brightness is non-linear. Norman R. Pogson has invented the accurate brightness classification system, that is magnitude. Magnitude is a numerical scale to describe brightness of each star appeared in the sky. This theory led to a scale in which any difference of 1 magnitude between two stars indicates a constant ratio between their brightnesses. By the modern definition, a difference of 5 magnitudes corresponds exactly to a factor of 100 in brightness, so a difference of 1 magnitude corresponds exactly to a brightness ratio of $100^{0.2} \approx 2.512$. Thus, a second-magnitude star appears about 2.512 times fainter than a first-magnitude star. There are two types of magnitudes, i.e. apparent magnitude and absolute magnitude. The apparent magnitude is the number that is a determination of its brightness as seen by an observer on Earth. We can calculate from the following equation:

$$m = -2.5 \log f + constant, \tag{2.8}$$

where m is the apparent magnitude, f represents the flux density of star in $\mathrm{W\,m^{-2}}$ and $constant$ corresponding to the zero point.

The zero point is used to calibrate the magnitude of the sample galaxies which can be obtained from the difference between the instrumental magnitude of each stars appeared within the data images and the magnitude from database for each filter. The zero point is constant for all reference stars that appear in the same images. Because each star has

different distance from Earth. If we want to compare the actual brightness of the star, we must be considered the brightness of the star at equal distance. So, astronomers have defined the standard distance is 10 pc. At standard distance of 10 pc, the absolute magnitude can be calculated from the equation:

$$M = m - 5\log d + 5, \tag{2.9}$$

where M refers to the absolute magnitude, m represents the apparent magnitude and d represents the distance from the earth in the unit of pc.

The color index is a numerical expression that determines the color of stars or sky objects, corresponding to their temperatures and spectral types. To measure the index, we can observe the magnitude of an object through two different filters, such as V and R or B and V, where V is magnitude in V filter, R is magnitude in R filter, and B magnitude in B filter. The difference in magnitudes found with these filters is called the $V - R$ or $B - V$ color index, respectively. As stellar magnitudes decrease with increasing brightness, a star with a smaller B–V color index is bluer than a star with a larger value of B–V (Carroll and Ostlie, 2014).

2.5 Surface Brightness of Galaxies and B_{25} Isophotes

For extended objects, the surface brightness can be defined as the flux density per unit solid angle. The surface brightness is independent of distance. In the figure 2.9, the flux density come from an area A is inversely proportional to the distance squared (r^2). But the surface brightness remains constant because of the solid angle subtended by the area A is also inversely proportional to the distance squared.

Giant galaxies with high luminosity also have high surface brightness, that is a high flux density per unit solid angle. This lends them their impressive appearance relative to the night sky. While dwarf galaxies are commonly of low surface brightness, they look rather diffuse, and can be difficult to see against even the faint sky foreground glow from our night time atmosphere (Phillipps, 2005).

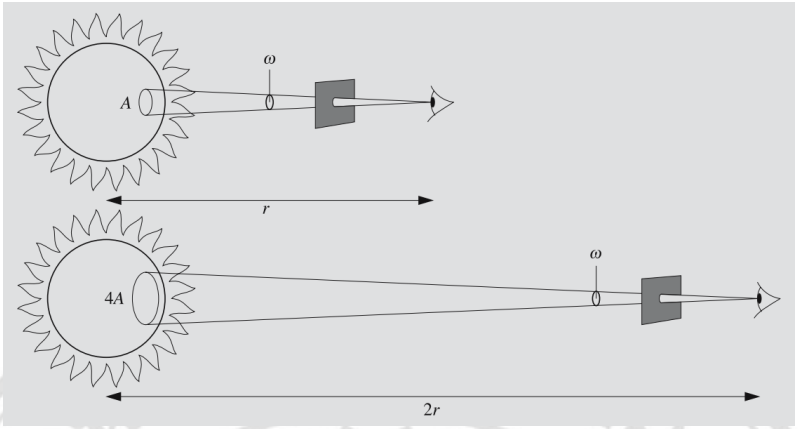

Figure 2.9: The diagram of the equal observed solid angle. Although the distance is increased, the surface brightness remains constant. (Karttunen et al., 2007).

The standard unit of surface brightness is W m^{-2}. However we always use solar luminosity per square parsec (L$_\odot$ pc^{-2}) or magnitudes per square arcsecond (mag arcsec^{-2}) as well. The sun has surface brightness, for example, of about $\mu_B = 27.05$ mag arcsec^{-2} (Phillipps, 2005) and also correspond to blue absolute magnitude of the sun is $M_B = 5.48$. Generally, galaxies have the most star distribution at the center of them. Therefore, the surface brightness of the galaxies will be correlated with the radial distance. For the disk of face-on spiral galaxies, the exponential intensity profile will be used to fitted the surface brightness distribution as shown in equation 2.10.

$$I(R) = I_0 \exp\left(\frac{-R}{H_R}\right), \tag{2.10}$$

where I_0 is the central region intensity, $I(R)$ corresponds to the intensity at the radial distance R, and H_R is the scale length of the disk along the midplane. We can derive the surface brightness in term of magnitudes, that becomes

$$\mu(R) = \mu_0 + 1.086R/H_R. \tag{2.11}$$

For the bulges of spiral galaxies, and for large eliiptical galaxies, are often assume to obey the $R^{1/4}$ law or de Vaucouleurs profile. That is the surface brightness as a function of $R^{1/4}$. We can be written the profile as

$$I(R) = I_e \exp\left(-7.67\left[\left(\frac{R}{R_e}\right)^{1/4} - 1\right]\right), \tag{2.12}$$

and in term of magnitudes, that becomes

$$\mu(R) = \mu_e + 8.33\left[\left(\frac{R}{R_{\rm e}}\right)^{1/4} - 1\right], \tag{2.13}$$

where $R_{\rm e}$ represents the effective radius, the projected radius within which a half of the galaxy's total flux density, I_e is the intensity at radius $R_{\rm e}$, and μ_e refers to the effective surface brightness at radius $R_{\rm e}$ (Carroll and Ostlie, 2014; Phillipps, 2005).

The brightness of the sky background is the problem that occur when we are observing the faint galaxies. The glowing night sky has an average surface brightness of about $\mu_{\rm sky} = 22\,\text{B-mag}\,\text{arcsec}^{-2}$ (Carroll and Ostlie, 2014). In general, galaxies are faint objects and difficult to determine their boundaries. Moreover, galaxies have variety of morphology, the inclined orientation plane and the non-uniform distribution of brightness. Thus, magnitude measurement of the galaxies in this research is needed to define the limit of the brightness distribution of galaxies at magnitude of the B-band filter equal to $25\,\text{mag}\,\text{arcsec}^{-2}$ (B_{25} isophote) around the center of the galaxy (de Vaucouleurs et al., 1976). This isophote (contours of constant surface brightness as shown in figure 2.10) can be obtained from the Extended Surface Photometry (`ESP`) package of `Starlink`. We can identify three parameters; semi-major axis (a), eccentricity (e) and position angle (PA) to define the size of the aperture for all filters which will be used to measure the magnitude and the flux count of galaxies.

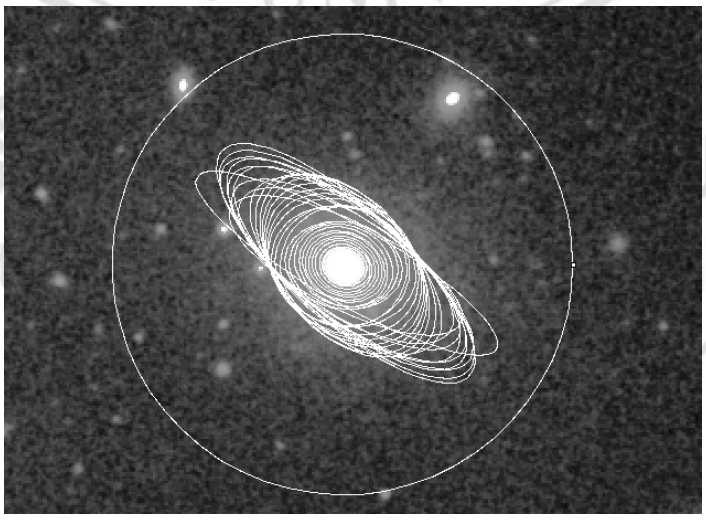

Figure 2.10: Isophotes of the sample galaxy from the `Starlink` software.

2.6 Galactic Extinction

From equation 2.9 shows that when the distance increases, resulting in apparent magnitude is increased (brightness is decreased). If the space between the observer and the radiation source is not thoroughly empty, but fills with interstellar or intra-galactic medium. Some of the radiation is absorbed by these matter and released energy at other wavelengths, which are scattered out of the line of sight, or outside of the waveband defining the magnitude. All these radiation losses are called the extinction. Assume we have a star radiate a luminosity L_0 in to a solid angle in some wavelength range. Since the radiation is absorbed and scattered by the medium, the observed luminosity L will be decreased with increasing distance. We can express the observed luminosity as

$$L = L_0 e^{-\tau}, \tag{2.14}$$

where τ is the optical thickness of the medium between the observer and the radiation source which is directly proportional to the distance. Similarly, the flux density is decreased with increasing distance. We need the flux density at a distance of 10 pc for the absolute magnitude. So, the equation for calculation of the absolute magnitude will be expressed as

$$M = m - 5\log\frac{r}{10\text{pc}} - A, \tag{2.15}$$

where $A \geq 0$ is the extinction in magnitude due to the all medium between the observer and the source.

2.7 Hα Equivalent Width ($EW(\text{H}\alpha)$) and Star Formation Rate

Young ($< 4 \times 10^6$ yrs), massive ($> 8\text{M}_\odot$) star formation activity in galaxies are indicated by the Balmer flux of Hα emission arising from HII regions (Kennicutt, 1998; Kennicutt and Kent, 1983). Because of the emission is not limited by absence of gas in the regions where hot stars are found, the amount of Hα emission is a function of the amount of ionized gas that is excited by the ultraviolet radiation (Cohen, 1976). The Hα emission can be determined in term of equivalent width (EW), and directly dependent on the number of OB stars . Typically, OB stars are massive stars with high surface temperature, that are formed not long ago and have a short-lived. This is consistent with a lot of

gas found in the late-type galaxies, particularly in the galactic disks (Pohlen et al., 2010; Boselli et al., 2002), which hydrogen gas is the main raw material for star formation. Electrons of hydrogen atoms around the young massive stars are excited by ultraviolet emitted from the OB stars and re-emitted the energy as the visible wavelength of Balmer series in narrow-band of Hα ($\lambda = 6563$ Å). Therefore, the Hα emission line provides a closely instantaneous determine of the star formation rate, independent of the former star formation history (James et al., 2005). The figure 2.11 shows the spectrum of a star-forming galaxy with Hα emission line. The measurement of $EW(\mathrm{H}\alpha)$ could be a good indicator for star forming regions within galaxies (Fossati et al., 2013; Kennicutt, 1998), that can be calculated by equation from Gavazzi et al. (2006) and Kriwattanawong et al. (2011). In addition, colors of galaxies also correlate with the $EW(\mathrm{H}\alpha)$ (Kennicutt and Kent, 1983) and can use to explain the evolution of galaxy and star formation.

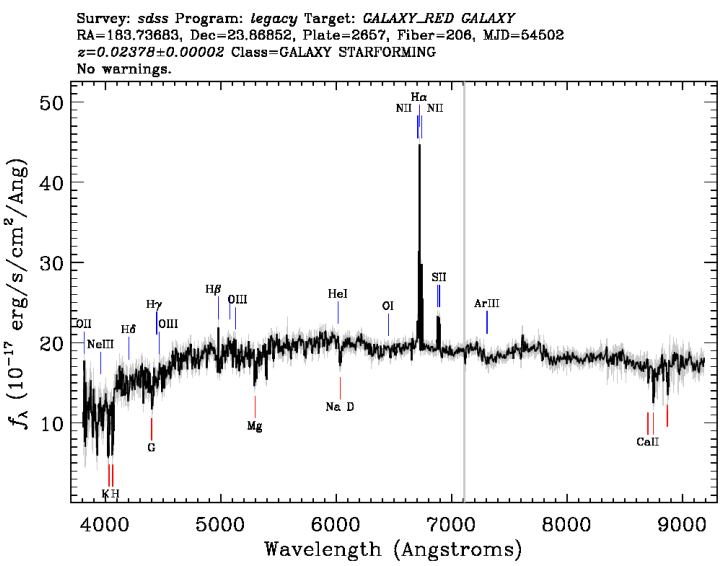

Figure 2.11: Available spectral line of 2MASX J12152202+2359376 from SDSS.

Star formation rate (SFR) is the number of star formed per unit time. This rate should be normalized to the galaxy mass or gas mass when comparing among different galaxies. Typically, the overall SFR in normal spiral and irregular galaxies is about $1 - 5\mathrm{M}_\odot\ \mathrm{yr}^{-1}$. But the SFR in dwarf irregulars may be as low as $6 \times 10^{-4}\mathrm{M}_\odot\ \mathrm{yr}^{-1}$. The SFR per galaxy mass slightly increases with later Hubble type due to the later types have relatively more gas than earlier types, while the SFR per unit gas mass is independent of

Hubble type (Elmegreen, 1998). The population synthesis models of Sandage (1986) indicated that the overall SFR in spirals and large irregulars may have been approximately constant over the last billion years. On the other hand, elliptical galaxies evidently had most of their star formation in the first billion years after their formation.

Star formation rate in the galaxies have been researched with various methods, especially, measurement of equivalent width of hydrogen alpha emission lines (e.g. Kennicutt and Kent, 1983; Young et al., 1996). Unfortunately, the measured Hα luminosity flux counts are typically contaminated with [N II] line counts. The [N II] lines are located two sides of the Hα line (λ 6563 Å) , at 6548 Å and 6583 Å. The bandwidth of the narrowband [S II] filter used in this research is 30 Å approximately. When we used [S II] filter to detect Hα emission line of the low redshift galaxies, the [N II] lines were included in the measured flux counts. So the [N II] components of the observed flux are needed to be removed before star formation rate can be calculated (Lee et al., 2009; James et al., 2005).

2.8 Galaxy Environments and Interactions

Dressler (1980) had studied galaxy populations in 55 rich clusters in order to describe the formation and evolution of various morphological type of galaxies. He found that the local galaxy density has correlated with the galaxy type, i.e. the elliptical and lenticular population were increased and a corresponding decrease in spirals with increasing density (see figure 2.12). These gradients in population result from lenticular galaxies when spirals are swept of their disk gas by an intra-galactic medium (Dressler, 1980). The gas from spirals can be removed by evaporation or ram pressure stripping that located in regions where gas temperature and density are too low, and then spirals will be transformed to lenticular. So, the large number of elliptical and lenticular could be found in very high density regions and the predominance of spiral galaxies at very low density. From the hypothesis of spiral sweeping, it is demonstrated that the correlation between morphological type and local density reflects the long time scale associated with the disk component formation of galaxies (Dressler, 1980). This is a result of different formation mechanisms or different evolutionary traces for galaxies in different environment interactions (Phillipps, 2005).

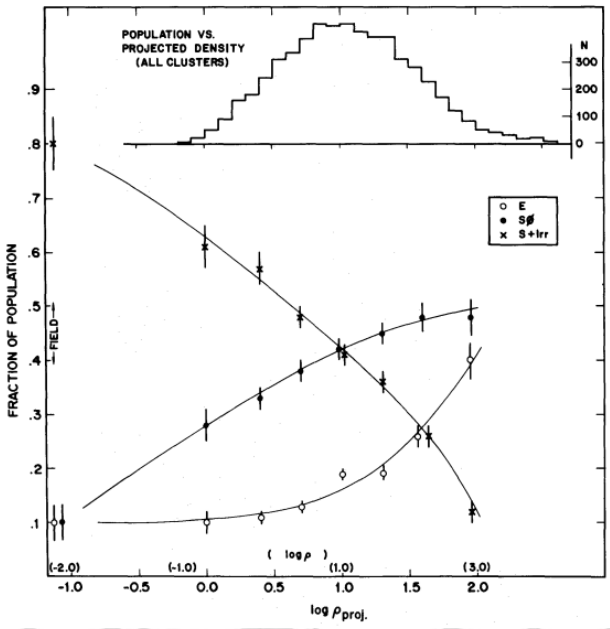

Figure 2.12: The morphology-density relation demonstrated by Dressler (1980).

There are many previous researches which studied the environmental effects on the galaxies in nearby cluster, e.g. Boselli and Gavazzi (2006), Fujita (2004) and Mihos et al. (1992). The difference of environment can affect the evolution of galaxies into various types. We now concisely review the physical processes which are believed to explain the galaxies interaction in dense environments consist of the gravitational interactions, including all tidal interactions (galaxy-cluster, galaxy-galaxy, and harassment) and the hydrodynamic interactions occurred between interstellar medium in galaxy and hot intra-galactic medium (ram pressure stripping, and viscous stripping).

2.8.1 Tidal interactions

Tidal interactions resemble the main morphological transformation mechanism of spirals to S0s. The efficient mechanism occurs in the high density environments. Tidal interaction induced star burst emission increases from lower to higher density of central galaxy. This can be interpreted that morphological transformation of the disc galaxies progresses more rapidly in the higher central galaxy density (Moss and Whittle, 2000). The indicator of tidal force interaction between galaxy-cluster, galaxy-group, and galaxy-galaxy is the circumnuclear emission in the galaxy either with bar structures or morphological disturbances.

1) Galaxy-Galaxy tidal interaction

Tidal interaction between pairs of galaxies acts on gas, dust, stars, and dark matter. The efficiency depends on ability of gravitational bounding, which cause of morphological transformation. Tidal interactions can remove the mass in the galactic halo and efficiently perturb the gas around the plane of galaxy more than molecular gas trapped in the potential well. Star formation was compared between observations (e.g. Keel et al., 1985) and simulations (e.g. Mihos et al., 1992) of tidal interaction. It was found that nuclear activities dramatically increase, while they slowly increase in the disk. So, the tidal interaction in galaxy-galaxy are boosted in the dense core of cluster galaxies. The interactions capably generate enough gas flow from the disk to the center region (Boselli and Gavazzi, 2006). Although, tidal interactions among the cluster galaxies occur frequently, but it will be happened in a short timescale. Thus, the perturbation effects are not very severe.

2) Tidal interaction among galaxies and the cluster potential well

The mass approximation of galaxy clusters is $10^{14}\ M_{\odot}$. The tidal interaction between galaxies and the cluster potential well can efficiently perturb the galaxies in the cluster, inducing the gas flow, star formation in the disk and bar formation. If the disk plane is parallel with respect to the orbital plane, the structure of the disk can be disturbed and formed the spiral arms. While the disk plane is perpendicular or incline relative to the orbital plane, it can be led to build the bulge of galaxies. The model of Fujita (1998) has shown that the tidal force of the cluster potential well can accelerate molecular cloud from the disk falls into the cluster center. The increase of kinetic pressure in the interstellar medium can induce star formation. The tidal interactions between galaxy and galaxy cluster induce nuclear activities to increase. While the amount of gas that used in star formation decreased. In other words, the gas in the interstellar medium can be consumed dramatically by a process of tidal interactions between galaxies and galaxy clusters to form young stars (Boselli and Gavazzi, 2006).

2.8.2 Ram pressure

Gunn and Gott (1972) suggested that the interstellar medium could be eliminated from the galaxies that are moving at velocity about 1,000 $\mathrm{km\,s^{-1}}$ pass through the hot and dense inter-galactic medium. The mechanism is known as ram pressure stripping. The interstellar medium will be removed more effectively by the pressure, especially H I atoms in the galaxy at velocity vicinity to the velocity dispersion of galaxy cluster and if the ram pressure able to overcome the gravitational pressure that bound gas in the galaxy disk. It is transformation of spiral galaxy into lenticular or dwarf galaxy.

The efficiency of removing gas out of the galaxy based on the tilt of the galaxy disk plane relative to the trajectory around the galaxy cluster. That is gas in face-on galaxies could be removed more easily than an edge-on galaxy. Moreover, the size of the galaxy also affects too. Because the small galaxies have shallower potential well than the larger galaxy, the dwarf galaxy was perturbed by ram pressure more than the large galaxies which have strengthened potential well enough to preserve the gas from ram pressure stripping.

Before the gas is eliminated from the galaxy, ram pressure compresses the medium in front of the galaxy and creates a bow shock and the low density gas tail behind the galaxy similar to comets. Only the molecular clouds with surface density less than $4 \times 10^{-3}\ \mathrm{g\,cm^{-2}}$ are swept out from the galaxy. While molecular clouds are dense in $10^{-2}\ \mathrm{g\,cm^{-2}}$ are not much affected. Then gas is compressed into molecular clouds can collapse easily. The increase of star formation rate can be happened (Boselli and Gavazzi, 2006).

Considering the short timescale (about 10^8 yrs) for a rich-dense galaxy cluster, star formation activity can be increased up to twice as much. But considering the long timescale, elimination of H I sources and fuel that consume in star formation activities in the early period will be decreased the star formation rate in the long period. So, the reduction of the molecular clouds of the galaxy was expected from the gas consuming in star formation activity increased, but is not the result of ram pressure stripping. It is interesting that the rise of star formation is increased during the movement through the outskirts of the galaxy cluster that is a lower density of inter-galactic medium than the center of cluster.

2.8.3 Galaxy harassment

Previous research has demonstrated that the evolution of the cluster galaxies that are controlled by the combine of two factors; galaxy-galaxy encounter closely in the 50 kpc with high speed and interactions of potential energy of all galaxy clusters. The galaxy harassment or high velocity encountering of galaxies depends on the frequency of collisions, the severe of each collision, the tidal field strength of the cluster and distribution of potential energy in the galaxies. The harassment is one of several morphological transformation mechanisms. The elongated orbit galaxies are affected by harassment greater than circular orbit galaxies. The encounter heats up stars in the galaxy, causes the velocity dispersion to increase and the angular momentum to decrease. As a result, the gas sinks to the galaxy center (Moore et al., 1996).

The bright disk galaxies and low mass system have difference of evolution depended on the depth of the potential wells and disk scale length. The bright disk galaxies are relatively stable against harassment. But the low mass galaxies are severely disturbed by the interaction, because of the low density core. As a result, the central molecular gas was collected and heated up. So the encounter probabilities and star formation activities will be increased (Boselli and Gavazzi, 2006).

The mechanism is used to describe the distortion of the galaxy and contribution of star formation in spiral galaxy that fall into galaxy cluster. The mechanism induces gas compression at high pressure environment and tidal compression by the galaxy cluster. These will encourage the star burst but the mechanisms do not change the galaxy morphology and effect of distorted blue galaxies in the clusters. Although direct merger is usually rare, all of galaxy encounters the other galaxies with high speeds closely every one time per 1 billion years, at a distance separation within 50 kpc. The mechanism could drive the star burst and evolution of galaxies rapidly. The high resolution numerical model of galaxy harassment showed the damage caused by closed encounters (Moore et al., 1996).

2.8.4 Viscous stripping

The viscous stripping is a mechanism that can be removed gas from cluster galaxies. If the galaxy contains relatively high density cool interstellar medium and moving at high

velocity through the inter-galactic medium. This situation is sufficient to strip off the outer surface of interstellar medium due to viscosity momentum. The rate of stripping depends on nature of motion. Viscous stripping will be the laminar for small galaxies. Whereas, for large galaxies, the viscous stripping will be a turbulent similar to the merging galaxy (Boselli and Gavazzi, 2006).